Stein, W. H., and Moore, S. (1963), *Methods Enzymol. 6*, 820.
Takahashi, M., and Westhead, E. W. (1971), *Biochemistry 10*, 1700.
Tanford, C. (1961), Physical Chemistry of Macromolecules, New York, N. Y., John Wiley and Sons.
Truffa-Bachi, P., van Rapenbusch, R., Janin, J., Gros, C., and Cohen, G. N. (1968), *Eur. J. Biochem. 5*, 73.
Truffa-Bachi, P., van Rapenbusch, R., Janin, J., Gros, C., and Cohen, G. N. (1969), *Eur. J. Biochem. 7*, 401.
Wampler, D. E., Takahashi, M., and Westhead, E. W. (1970), *Biochemistry 9*, 4210.
Warburg, O., and Christian, W. (1942), *Biochem. Z. 310*, 384.
Weber, K., and Osborn, M. (1969), *J. Biol. Chem. 244*, 4406.
Yphantis, D. A. (1964), *Biochemistry 3*, 297.

Sedimentation Equilibrium of Protein Solutions in Concentrated Guanidinium Chloride. Thermodynamic Nonideality and Protein Heterogeneity†

Petr Munk and David J. Cox

ABSTRACT: The theory of sedimentation equilibrium of heterogeneous nonideal solutes has been reviewed. It has been shown by simulation experiments that conventional treatments of experimental data neglecting the nonideality and heterogeneity may yield erroneous molecular weights, particularly when the low-speed technique is used. A simple procedure for the treatment of experimental data has been designed to eliminate these errors. The validity of the new procedure has been successfully tested on solutions of several proteins in 6 M guanidinium chloride. A density gradient is formed in complex solvents during centrifugation. The effect of this gradient on sedimentation equilibrium of macromolecular solutes has been studied in detail and has been shown to be negligible for protein solutions in guanidinium chloride. Differential evaporation from solution and solvent may produce large errors in measurements of solute concentration in a synthetic boundary cell. These errors can be detected and eliminated by simple modifications of the experimental technique.

Native proteins frequently consist of several polypeptide chains. Guanidinium chloride at high concentrations disrupts the noncovalent interactions that maintain the conformations of the individual chains and hold the chains together in the native structure. If a mild reducing agent is present, inter- and intrachain disulfide bonds are also broken, and the original aggregate is usually converted to a collection of separate chains, each of which exhibits the hydrodynamic and thermodynamic behavior of a statistical coil (Tanford *et al.*, 1967; Kawahara and Tanford, 1966; Lapanje and Tanford, 1967).

Sedimentation equilibrium experiments with proteins in a solution containing concentrated guanidinium chloride and a moderate amount of an appropriate mercaptan are used frequently for measurement of the average molecular weight of the subunits (Green and McKay, 1969; Truffa-Bachi *et al.*, 1969). These systems do, however, display some complexities which are frequently neglected in subunit studies because they are not commonly met in other contexts by protein chemists. Many native proteins behave nearly ideally at low concentration and the neglect of nonideality is not very damaging except in rather sophisticated studies of associating systems. On the other hand, the virial coefficients of proteins in guanidinium chloride are at least an order of magnitude higher than those of native globular proteins in normal solvents (Lapanje and Tanford, 1967; Castellino and Barker, 1968). If the effect of nonideality is ignored, erroneous conclusions may be drawn from sedimentation equilibrium measurements.

It is well known (Tanford, 1961) that the common treatments of sedimentation equilibrium data yield straight lines for ideal homogeneous solutes and curved plots for nonideal as well as heterogeneous samples. Experiments that produce reasonably straight lines may be described as indicating that the samples concerned are homogeneous within the limits of the technique. It is, however, not usually clear how broad are the limits of the technique. Nonideality tends to mask curvature due to heterogeneity. In dealing with a protein composed of subunits, it is important to ask whether sedimentation equilibrium in concentrated guanidinium chloride can be expected to produce any useful information bearing on the identity or nonidentity of subunits.

A sedimentation equilibrium experiment yields apparent molecular weights over a range of solute concentrations, and, for a homogeneous solute, a single experiment can, in principle, provide the information needed to eliminate the effect of nonideality. The problem may be approached by plotting the apparent molecular weight against concentration and obtaining the true value by extrapolation to infinite dilution (Seery *et al.*, 1967, 1970). If such a procedure is to be of practical use, it must not demand data more precise than those provided by real experiments. Experimental errors that tend to produce spurious curvature in the data plots must be eliminated. It is also necessary to know which average of molecular weight is produced by any given extrapolation procedure if the solute happens to be heterogeneous. Alternatively, one of the "ideal" molecular weight moments can be calculated point by point along the solution column (Roark and Yphantis, 1969). If the solute is homogeneous, the ideal moments are essentially independent of concentration, and the values ob-

† From the Department of Chemistry and Clayton Foundation Biochemical Institute, The University of Texas at Austin, Austin, Texas 78712. *Received July 7, 1971.*

tained at different points in the cell can be averaged. The plotting procedure and the ideal moment method can be made to provide equivalent information, and the two techniques require data of comparable precision.

Concentrated guanidinium chloride is a two-component solvent. The interpretation of sedimentation equilibrium experiments in two-component solvents can be ambiguous unless certain features peculiar to such systems are taken into account. Preferential solvent binding has been described theoretically in great detail (Casassa and Eisenberg, 1964). Data in the literature can supply reasonable estimates of the importance of this effect for proteins in guanidinium chloride, and experimental procedures are available for dealing rigorously with it (Reisler and Eisenberg, 1969). However, an additional difficulty can arise in a two-component solvent. Redistribution of the solvent components at sedimentation equilibrium produces a density gradient. In the case of concentrated guanidinium chloride at moderate rotor speeds, it is not immediately obvious that the equilibrium density gradient is so small as to be negligible in the treatment of the data, especially a treatment which stresses the variation of the apparent molecular weight along the solution column.

In this paper, we present simulated and experimental data which show that, although the nonideality anticipated for proteins in guanidinium chloride may not be visually striking, it is very likely, if neglected, to produce important errors in sedimentation equilibrium experiments. We advocate a procedure which allows the true molecular weight and an estimate of the virial coefficient to be extracted from the data. The procedure requires no more experimental data than a conventional measurement, and the computation is not so cumbersome as to preclude its use in routine work. The density gradient effect is explicitly shown to be immeasurably small for guanidinium chloride solutions under the usual experimental conditions. Sedimentation equilibrium in guanidinium chloride is shown to be an exceedingly insensitive way to detect subunit heterogeneity. Careful treatment of the data produces only very tentative information on this point; casual examination produces no information at all. In addition we comment on a few points of experimental technique which require some attention if certain misleading artifacts are to be avoided.

Theoretical

One-Component Solvents. The condition for equilibrium in ultracentrifuge was expressed (Goldberg, 1953) as

$$M_i(1 - \bar{v}_i\rho)\omega^2 r = \sum_{k=1}^{K} (\partial\mu_i/\partial c_k)_{T,p,c_j}(\mathrm{d}c_k/\mathrm{d}r) \qquad i = 0, 1, \ldots, K \quad (1)$$

Here M_i, $\bar{v}_i$, μ_i, and c_i are the molecular weight, partial specific volume, chemical potential, and concentration in grams per milliliter of solution of the ith component, respectively. The angular velocity of the rotor is ω; r is the distance from the rotational axis, p is the pressure, T is the absolute temperature, and ρ is the density of the solution. When applying eq 1 to heterogeneous solutes in simple solvents, index 0 will be used to denote solvent, and

$$c = \sum_{i=1}^{K} c_i$$

will be the total concentration of solutes. For simplification, we will assume that the $\bar{v}_i$'s are independent of the pressure and of the composition of the system, and that all solute $\bar{v}_i$'s are equal: $\bar{v}_i = \bar{v}_1$.

Then the density of the solution ρ may be expressed as

$$\rho = \sum_{i=0}^{K} c_i = \rho_0 + (1 - \bar{v}_1\rho_0)c \quad (2)$$

$$1 - \bar{v}_1\rho = (1 - \bar{v}_1\rho_0)(1 - \bar{v}_1 c) \quad (3)$$

As in previous treatments (Goldberg, 1953; Fujita, 1962), we will express the chemical potential by means of the activity coefficient, y_i, based on c_i units. Further, we will expand the ln y_i into a series using binary interaction coefficients B_{ik}. Finally, we will assume that all B_{ik} are identical (Fujita, 1962).

$$\mu_i - \mu_{i0} = RT[\ln c_i + \ln y_i] = RT[\ln c_i + M_i \sum_{k=1}^{K} B_{ik}c_k + \ldots] = \quad (4)$$

$$= RT[\ln c_i + BcM_i + \ldots]$$

The second index zero of μ_{i0} refers to the standard state; R is the gas constant. It is worthwhile to mention that these assumptions lead to the following form of dependence of osmotic pressure, π, on concentration.

$$\pi/cRT = 1/\bar{M}_n + c(B/2 + \bar{v}_1/2\bar{M}_n) + \ldots \quad (5)$$

Here $\bar{M}_n$ is the number-average molecular weight, defined together with other averages in the usual way.

$$\bar{M}_n = \sum_{i=1}^{K} c_i / \sum_{i=1}^{K} c_i/M_i \quad (6a)$$

$$\bar{M}_w = \sum_{i=1}^{K} M_i c_i / \sum_{i=1}^{K} c_i \quad (6b)$$

$$\bar{M}_z = \sum_{i=1}^{K} M_i^2 c_i / \sum_{i=1}^{K} M_i c_i \quad (6c)$$

Substituting eq 3 and eq 4 into eq 1 results in

$$M_i(1 - \bar{v}_1\rho_0)(1 - \bar{v}_1 c)\omega^2 r = RT[(\mathrm{d}c_i/\mathrm{d}r)/c_i + M_i B(\mathrm{d}c/\mathrm{d}r) + \ldots] \quad (7)$$

Multiplication by c_i and summation over $i = 1, 2, \ldots, K$ then gives

$$c\bar{M}_w(1 - \bar{v}_1\rho_0)\omega^2 r = RT(\mathrm{d}c/\mathrm{d}r)[1 + c\bar{M}_w(B + \bar{v}_1/\bar{M}_w) + \ldots] \quad (8)$$

where $(1 - \bar{v}_1 c)^{-1}$ has been expaned into binomial series and the term $\bar{v}_1 c$ combined with $Bc\bar{M}_w$.

In the case of ideal solutions, $c\bar{M}_w(B + \bar{v}_1/\bar{M}_w)$ is negligible throughout the cell, and relations 7 and 8 are used in a number of ways to calculate different averages of molecular weight. Thus, the slope of a plot ln c *vs.* r^2 at sedimentation equilibrium gives (Tanford, 1961) $\bar{M}_w^r$

$$\mathrm{d}\ln c/\mathrm{d}(r^2) = \bar{M}_w^r(1 - \bar{v}_1\rho_0)\omega^2/2RT \quad (9)$$

where $\bar{M}_w^r$ is the value of $\bar{M}_w$ at radial distance r. The plot is linear for a homogeneous solute. Similarly, a plot of $(dc/dr)/r$ *vs.* c has a slope $\bar{M}_z^r(1 - \bar{v}_1\rho_0)\omega^2/RT$ and is linear for a homogeneous solute (Tanford, 1961). Both these plots are curved up for polydisperse solutes, as $\bar{M}_w^r$ and $\bar{M}_z^r$ increase toward the bottom of the cell.

Alternatively, eq 8 may be integrated over the whole column in the cell giving

$$\bar{M}_w = (c_b - c_m)2RT/(1 - \bar{v}_1\rho_0)(r_b^2 - r_m^2)\omega^2 c_0 \quad (10)$$

$$\bar{M}_z = [(dc/dr)_b/r_b - (dc/dr)_m/r_m]RT/(1 - \bar{v}_1\rho_0)\omega^2(c_b - c_m) \quad (11)$$

where indices b and m refer to the bottom and meniscus of the solution column (Tanford, 1961).

For nonideal systems, the above treatments yield values which depend on the initial concentration of the solution. In usual procedures (Deonier and Williams, 1969), the apparent value of $\bar{M}_w$ is calculated from eq 10 for several concentrations. The true value of $\bar{M}_w$ and B is then obtained from a plot of the apparent molecular weight against the initial concentration c_0, or against the related quantity $(c_m + c_b)/2$. The obvious disadvantage of such a procedure is a necessity of performing several time-consuming measurements of sedimentation equilibrium for each sample. However, in any one sedimentation equilibrium experiment, the concentration of the solute varies continuously from point to point in the cell. Thus, the apparent molecular weight $\bar{M}^r$ could be obtained as a function of concentration in a single experiment and could, in principle, be used for finding the true molecular weight and the virial coefficient (Seery *et al.*, 1967, 1970).

Rearrangement of eq 8 yields

$$1/\bar{M}_{app}^r \equiv (1 - \bar{v}_1\rho_0)\omega^2 cr/RT(dc/dr) = 1/\bar{M}_w^r + c(B + \bar{v}_1/\bar{M}_w^r) + \ldots \quad (12)$$

Generally, of course, eq 12 does *not* define a linear relation between reciprocal apparent molecular weight and concentration in the cell, because $\bar{M}_w^r$ is changing with the position in the cell for heterogeneous solutes.

For a homogeneous solute, however, the plot of $1/\bar{M}_{app}$ *vs.* c is linear and yields $1/\bar{M}_w$ and $B + \bar{v}_1/\bar{M}_w$ as intercept and slope, respectively. The coefficient at c is exactly twice the corresponding one for osmotic pressure measurement (compare eq 5).

For heterogeneous solutes, the plot is curved; extrapolating the curve to vanishing concentration is not advisable, because the curve does not correspond to any physical situation beyond the point c_m. Let us therefore calculate the slope and intercept of a tangent to the above dependence at the point c^r. Simple, but lengthy calculation will show that the tangent may be expressed as

$$1/\bar{M}_{app}^r = \{\bar{M}_z^r/\bar{M}_w^{r2} + \bar{v}_1c^r[(\bar{M}_z^r/\bar{M}_w^r - 1) - c^r(B\bar{M}_w^r + \bar{v}_1)/(1 - \bar{v}_1c^r)]/\bar{M}_w^r(1 - \bar{v}_1c^r)\} + c\{(B + v_1\bar{M}_z^r/\bar{M}_w^{r2})/(1 - \bar{v}_1c^r) - (\bar{M}_z^r/\bar{M}_w^r - 1)/c^r\bar{M}_w^r(1 - \bar{v}_1c^r)^2\} \quad (13)$$

Here the upper index r refers to the values at the point where the tangent was drawn. Equation 13 is the exact equation for the tangent, provided that the series expression in eq 4 is truncated after the term BcM_i.

Before analyzing eq 13 it should be noted that the term $(1 - \bar{v}_1c^r)$ is typically larger than 0.99 (c^r is in g/ml). Substituting it by unity would greatly simplify eq 13. The first braces in eq 13 encompass the expression for the intercept of the tangent. The second term in the intercept is typically more than two orders of magnitude less than the first one, and is completely negligible. Thus, the intercept gives the value $\bar{M}_z^r/\bar{M}_w^{r2}$.

The second braces in eq 13 express the slope of the tangent. The first term in the slope is due to nonideality, while the second term is a measure of heterogeneity. The contribution of $v_1\bar{M}_z^r/\bar{M}_w^{r2}$ to the nonideality term is immeasurably small in most circumstances. The second term is inversely proportional to c^r and may therefore predominate at low concentrations such as are typical for high-speed equilibrium experiments. Thus, the slope tends to be smaller than the virial expression $B + \bar{v}_1/M$ if the sample is even only marginally heterogeneous.

The molecular weight average $\bar{M}_z^r/\bar{M}_w^{r2}$ is one of the "ideal" molecular weight moments (Roark and Yphantis, 1969). In principle, tangents to the plot of $1/M_{app}$ *vs.* concentration could be constructed at various points along the curve, and the intercepts of the tangents would yield $\bar{M}_z^r/\bar{M}_w^{r2}$ as a function of position in the cell. Real data are not likely to be precise enough to make this a practical procedure unless the data are smoothed. However, for moderately heterogeneous samples, the unsmoothed data can be fit by least squares to a straight line. As will be shown below, the intercept of such a straight line often lies close to $\bar{M}_z/\bar{M}_w^2$ for the whole sample. The ideal moment can also be calculated at several positions along the solution column by measuring apparent values of $\bar{M}_z^r$ and $\bar{M}_w^r$ separately, point by point. The expression for $\bar{M}_z^r$ involves d^2c/dr^2 (Roark and Yphantis, 1969), and these second difference measurements, like the construction of the tangents given by eq 13, usually require smoothing of the data.

As eq 13 shows, sedimentation equilibrium for heterogeneous nonideal solutes yields rather complicated results. It is not immediately apparent how much the nonideality and heterogeneity would influence the quantitative data, how large the errors may be that are committed when they are neglected, or how precise the information obtained from the analysis of experimental data could be. To gain a better insight into these problems the sedimentation behavior of several model systems was simulated by computer.

Model systems which resembled proteins in 6 M guanidinium chloride were chosen. The temperature was said to be 20°; the solvent density, $\rho_0 = 1.16$ g/ml; and the specific volume of protein, $\bar{v}_1 = 0.730$ ml/g. The ends of a 3-mm solution column were placed at $r_b = 7.1$ cm and $r_m = 6.8$ cm. For homogeneous examples, the molecular weight chosen was 60,000. In heterogeneous examples, equal numbers of molecules with molecular weights $M_1 = 36{,}000$ and $M_2 = 72{,}000$ were stated to be present. For such a mixture, $\bar{M}_w = 60{,}000$, $\bar{M}_z = 64{,}800$ and $\bar{M}_w^2/\bar{M}_z = 55{,}556$. The heterogeneous model was intended to represent a protein composed of two different kinds of subunits; the system was very heterogeneous by the standards of protein chemists.

For nonideal examples we defined $B + \bar{v}_1/M = 1.77 \times 10^{-3}$ (mole ml)/g^2; this is the average value for about ten proteins in guanidinium chloride solutions according to the literature (Lapanje and Tanford, 1967; Castellino and Barker, 1968). The virial coefficients in the quoted papers are osmotic pressure coefficients with half the numerical value appropriate for sedimentation equilibrium. The above value may be con-

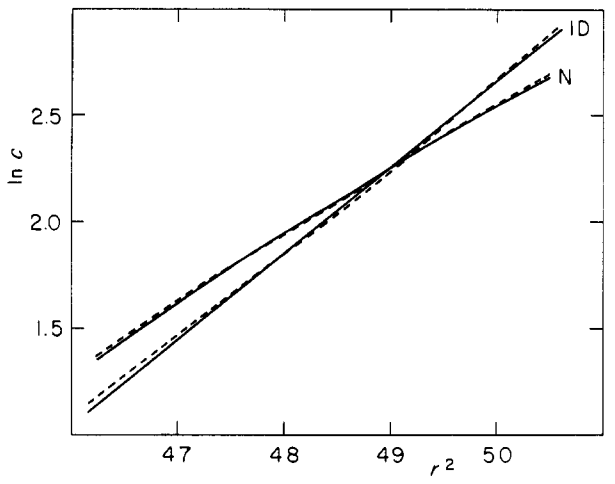

FIGURE 1: Simulated data for low-speed method, $\bar{M}_w$-type plot. Natural logarithm of concentration (in fringe units) as a function of r^2. Full lines for homogeneous solute, broken lines for heterogeneous solute. ID, ideal solution; N, nonideal solution.

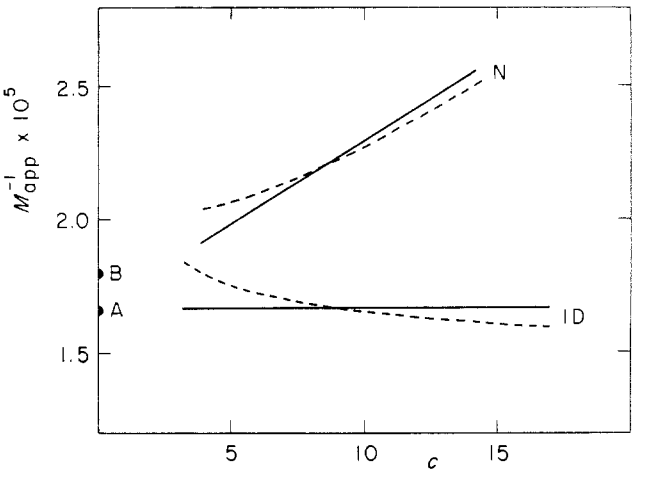

FIGURE 3: Simulated data for low-speed method. $1/M_{app}$ as a function of concentration (in fringe units). The same data and notation as in Figure 1. (A) True value of $\bar{M}_z/\bar{M}_w^2$ for homogeneous solute and (B) for heterogeneous solute.

verted by a proper factor (see below) to $B + \bar{v}_1/M = 6.16 \times 10^{-7}$ mole/g of fringe; fringes are convenient units of concentration in sedimentation experiments.

First, a group of experiments was simulated using a relatively high protein concentration and low speed (Richards and Schachman, 1959). The value chosen for total initial concentration was $c_0 = 8.2$ fringes (about 2.85×10^{-3} g/ml), and the speed was 14,000 rpm. The distribution of the solute at equilibrium was computed and the results were used as data for standard evaluation procedures.

In Figure 1, ln c is plotted *vs.* r^2 for ideal (denoted by ID) and nonideal (denoted by N) systems. Solid lines refer to homogeneous solutes and broken lines to heterogeneous ones. The average slope of the lines for the nonideal systems is much less than that of ideal ones; however, the curvature is not very impressive on casual examination. The curves for heterogeneous solutes differ only very little from corresponding curves for homogeneous solutes. The slight upward curvature tends to diminish the downward curvature caused by nonideality, but the curvature is still downward even for the very heterogeneous solute specified in the simulation.

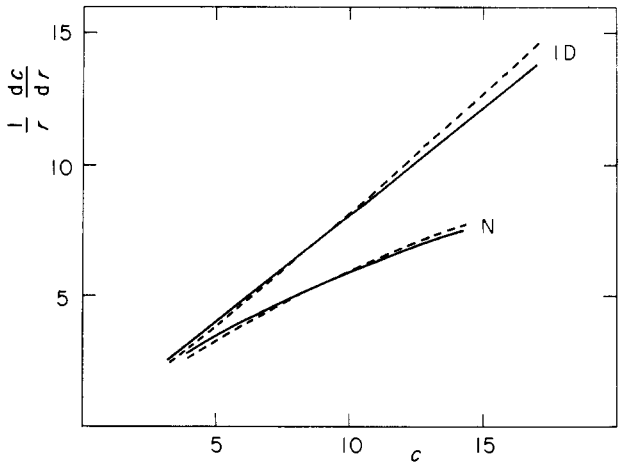

FIGURE 2: Simulated data for low-speed method, $\bar{M}_z$-type plot. $(dc/dr)/r$ as a function of concentration (in fringe units). The same data and notation as in Figure 1.

In Figure 2, the same data (labeled in the same way) are plotted as $(dc/dr)/r$ *vs.* c. In this plot there is a net difference in slopes for homogeneous and heterogeneous solutes due to the difference in $\bar{M}_z$. The effect of nonideality entirely masks that of heterogeneity. The curvatures are again only moderate.

In Figure 3, the same data are plotted as $1/\bar{M}_{app}$ *vs.* c. The points A and B denote the value of $\bar{M}_z/\bar{M}_w^2$ of the initial sample for homogeneous and heterogeneous solutes, respectively. As expected, the lines for the homogeneous solutes are straight and extrapolate toward the proper value of M. For heterogeneous solutes there is a considerable curvature in the plot and the average slope of the plot is much less (or more negative) than for corresponding homogeneous solutes; this is due to the second term in the slope part of eq 13.

In a real experiment there is inevitably some scattering of experimental points. Such scattering may obscure the slight curvature in plots in Figures 1 and 2. One may be tempted to draw a straight line through the points and evaluate the slope as for an ideal homogeneous solute. This may happen even for plots of the type in Figure 3. Although the curvatures are more pronounced in these plots, the experimental points will

TABLE I: Least-Square Estimates of Molecular Weights and Virial Coefficients in Low-Speed Experiments.

	$\bar{M}_w$[a]	$\bar{M}_z$[b]	$\bar{M}_w^2/\bar{M}_z$[c]	$B \times 10^7$[d]
Homogeneous				
True values	60,000	60,000	60,000	0.0[e] or 6.16[f]
Ideal	60,000	60,000	60,000	0.0
Nonideal	46,300	34,500	60,000	6.16
Heterogeneous				
True values	60,000	64,800	55,556	0.0[e] or 6.16[f]
Ideal	58,900	64,700	54,300	−1.72
Nonideal	45,800	37,000	54,600	4.52

[a] From slope of ln c *vs.* r^2 plot. [b] From slope of $(dc/dr)/r$ *vs.* c plot. [c] From intercept of $1/M_{app}$ *vs.* c plot. [d] From slope of $1/M_{app}$ *vs.* c plot. [e] For ideal system. [f] For nonideal system.

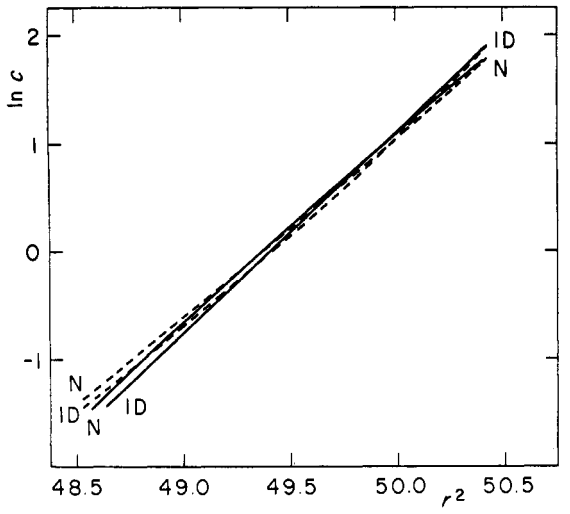

FIGURE 4: Simulated data for high-speed method, $\bar{M}_w$-type plot. Natural logarithm of concentration (in fringe units) as a function of r^2. Data truncated at concentration 0.25 fringe, the same notation as in Figure 1.

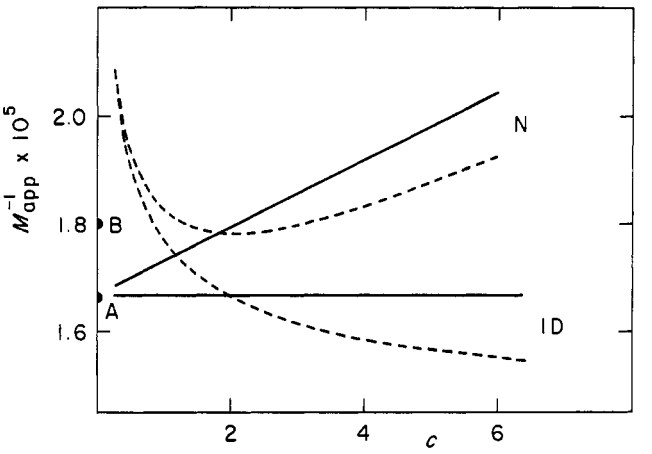

FIGURE 6: Simulated data for high-speed method. $1/M_{app}$ as a function of concentration (in fringe units). The same data as in Figure 4, notation as in Figure 3.

also be more widely scattered due to the expanded scale for $1/M_{app}$.

To simulate such a procedure we have calculated the least-squares straight lines through sets of points at equal intervals along the r coordinate in the cell. Then we have evaluated the various apparent averages of molecular weights and virial coefficients from the slopes and intercepts of the least-squares plots. The results of this procedure are summarized in Table I. For ideal systems, all three types of plot give reasonable results. However, only the $1/M_{app}$ plot signalizes the heterogeneity of the solute by an apparently negative virial coefficient. For the nonideal case, the ln c *vs.* r^2 plot and the $(dc/dr)/r$ plot give very low values of molecular weight, and the apparent value of $\bar{M}_z$ is less than that of $\bar{M}_w$. The $1/M_{app}$ plot gives values close to the values of the original sample in all cases. Again, the apparent value of virial coefficient is smaller for heterogeneous solutes than for homogeneous ones.

For the simulation of high-speed meniscus depletion experiments (Yphantis, 1964), we have chosen an initial concentration of 0.82 fringe (about 2.85×10^{-4} g/ml), and a rotor speed of 30,000 rpm. Other variables were the same as in the low velocity simulation. For the least-squares calculation, we have used only those points for which the concentration was larger than 0.25 fringe. This corresponds to the usual practice in high-speed experiments; the points at the low concentration end of the solution column with the highest error-to-value ratio are always rejected. The results are summarized in Figures 4–6 and in Table II.

Due to the low concentration and high velocity in high-speed experiments, the influence of nonideality is smaller and that of heterogeneity larger. The ln c *vs.* r^2 plots (Figure 4) seem almost identical for all four cases. Nevertheless, neglecting the nonideality causes a systematic error of about 6% in our particular case. The errors in $\bar{M}_z$-type evaluations are somewhat larger. The least-squares plots also gave small errors in $\bar{M}_w$ and $\bar{M}_z$ for the ideal heterogeneous solute. It should be noted that the size and direction of the errors in this case is somewhat arbitrary, since it depends on where the data are truncated and how much statistical weight is given to the various portions of the plot (*i.e.*, whether the points are taken at equal intervals along the concentration scale or along the scale of radial distances). The $1/M_{app}$ plot gives again the true values for the homogeneous solute. Heterogeneity, however, introduces a strong curvature and a negative slope. The least-squares calculation of the straight line parameters for this plot is rather arbitrary in the heterogeneous case.

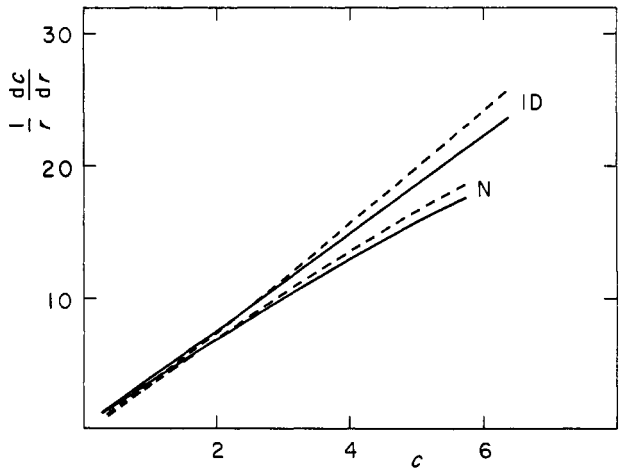

FIGURE 5: Simulated data for high-speed method, $\bar{M}_z$-type plot. $(dc/dr)/r$ as a function of concentration (in fringe units). The same data and notation as in Figure 4.

TABLE II: Least-Squares Estimates of Molecular Weights and Virial Coefficients in High-Speed Experiments.

	$\bar{M}_w$[a]	$\bar{M}_z$[b]	$\bar{M}_w^2/\bar{M}_z$[c]	$B \times 10^7$[d]
Homogeneous				
True values	60,000	60,000	60,000	0.0[e] or 6.16[f]
Ideal	60,000	60,000	60,000	0.0
Nonideal	56,600	49,900	60,000	6.16
Heterogeneous				
True values	60,000	64,800	55,556	0.0[e] or 6.16[f]
Ideal	57,300	65,300	52,400	−3.85
Nonideal	54,200	53,800	52,300	−1.11

[a–f] See footnotes in Table I.

Multicomponent Solvents. Until now, we have considered the sedimentation equilibrium of a solute in a simple, thermodynamically good solvent. In a multicomponent solvent such as guanidinium chloride solutions, several other effects come into play.

The effect of preferential sorption of solvent components on macromolecular solutes has been treated in detail (Casassa and Eisenberg, 1964). The effect is properly taken into account when the apparent specific volume of the solute, $\bar{v}_1^*$, calculated from density differences between solution and its dialysate is used instead of true $\bar{v}_1$. The definitions of both quantities are, respectively

$$\bar{v}_1 = [1 - (\partial\rho/\partial c)_{n,p,T}]/\rho_0 \quad (14a)$$

$$\bar{v}_1^* = [1 - (\partial\rho/\partial c)_{\mu,p,T}]/\rho_0 \quad (14b)$$

Here the index n refers to constant numbers of moles of other components, while index μ means constant chemical potentials. It was shown (Reisler and Eisenberg, 1969) that at least for two proteins (bovine serum albumin and rabbit muscle aldolase), the apparent specific volume $\bar{v}_1^*$ in 6 M guanidinium chloride is about 0.010–0.012 less than $\bar{v}_1$ in water solutions.

When the partial specific volumes of the components in a multicomponent solvent are not equal, then the solvent components are redistributed in the cell at sedimentation equilibrium and form a density gradient. Such a gradient influences the distribution of the macromolecular solute and, specifically, introduces some curvature into $\bar{M}_w$- and $\bar{M}_z$-type plots. Thus the evaluation of nonideality and heterogeneity, which is based on this curvature, may be affected. It will be shown that this effect is negligible for protein solutions in guanidinium chloride. Nevertheless, it can be significant in other systems, and so the treatment will be presented in detail.

Consider a two-component solvent. In the following, index 0 will be used for the major component of the solvent (*e.g.*, water) and index 2 for the other component (*e.g.*, salt, guanidinium chloride, etc.). The chemical potential of the salt may be expressed by eq 4 ($i = 2$). Introduction of eq 4 into eq 1 then yields after rearrangement

$$dc_2 = [c_2M_2\omega^2(1 - \bar{v}_2\rho)/2RT(1 + d \ln y_2/d \ln c_2)]d(r^2) \quad (15)$$

Due to the low molecular weight of the salt, the variation of the salt concentration in the cell is so small in all experiments at practical rotor velocities that the expression inside the brackets of eq 15 may be taken as constant for the purpose of integration. Integrated, eq 15 reads

$$c_2 = c_{20} + \Omega\omega^2(r^2 - \overline{r^2})/(1 - \bar{v}_2\rho_0) \quad (16a)$$

$$\Omega = c_{20}M_2(1 - \bar{v}_2\bar{\rho})(1 - \bar{v}_2\rho_0)/2RT(1 + d \ln y_2/d \ln c_2) \quad (16b)$$

$$\overline{r^2} = (r_b^2 + r_m^2)/2 \quad (16c)$$

where c_{20} and $\bar{\rho}$ refer to the initial concentration of salt and the initial density of the solution, respectively. Combination of eq 16a with eq 2 (written for salt, *i.e.*, $\bar{v}_1 \rightarrow \bar{v}_2$, $c \rightarrow c_2$) then yields for the local density

$$\rho = \bar{\rho} + \Omega\omega^2(r^2 - \overline{r^2}) \quad (17)$$

The parameter Ω may be found from the thermodynamic properties of the two-component solvent as given by eq 16b. (Note that M_2 for salts is the formula weight of the salt divided by the number of ions per formula.) However, the concentration dependence of the activity coefficient of salt, y_2, is usually not known for this concentration region. Therefore, a relatively easy experimental determination of Ω from an equilibrium experiment on the complex solvent itself is to be preferred (Hill and Cox, 1966).

Consider next the sedimentation equilibrium for a macromolecular homogeneous, ideal solute (index 1) in such a complex solvent. Equation 1 combined with 4 ($B = 0$), then simplifies to

$$M_1(1 - \bar{v}_1^*\rho)\omega^2/2RT = d \ln c_1/d(r^2) \quad (18)$$

Here the density, ρ, is given by eq 17 and increases continuously toward the bottom of the cell. Thus, the plot of $\ln c_1$ *vs.* r^2 has a continuously decreasing slope similar to the curvature introduced by a nonideal solute. $\bar{M}_w^r$ calculated from eq 9 is consequently only an apparent value. However, the apparent value approaches to the true value as r approaches to $\bar{r}$. Since $\bar{r}$ is close to the center of the column, the mean slope of the curve (or a straight line drawn through the scattered points) is close to the value expected for the case without a density gradient effect. The same applies to the $\bar{M}_z$-type plot $(dc/dr)/r$ *vs.* c. Thus, in an approximation that neglects heterogeneity and nonideality, the effect of density gradient may be neglected also.

When the plot of $1/M_{app}$ *vs.* c is to be employed, the quantity M_{app} must be redefined. The term $\bar{v}_1\rho_0$ in eq 12 should be replaced by $\bar{v}_1^*\rho$, where ρ is the position-dependent variable defined by eq 17. Otherwise, if $\bar{\rho}$ is used instead of ρ, then the new term, $2RT\bar{v}_1^*\Omega/\bar{M}_w^2c_1^r(1 - \bar{v}_1^*\bar{\rho})^2$, appears in the braces describing the slope part of eq 13 and the intercept is lowered also. Thus, neglecting the density gradient leads to overestimates of both the second virial coefficient and molecular weight and obscures the effect of heterogeneity. The question of immediate interest is how large these errors are for proteins in guanidinium chloride. We will see later that in this case, the effect is completely negligible.

Methods

Choice of Speed. The high-speed (Yphantis, 1964) and low-speed (Richards and Schachman, 1959) techniques have characteristic strengths and weaknesses for molecular weight determinations in concentrated guanidinium chloride. High-speed runs are done at low solute concentration, and so the errors in the uncorrected data due to nonideality are relatively small. On the other hand, the range of concentration covered in one run is relatively narrow, and extrapolation to remove the remaining error may be difficult to do precisely. Low-speed experiments are done at higher concentration and the apparent molecular weights are likely to differ substantially from the true values. However, the data can be made to cover a fairly broad range of solute concentration. Extrapolation to infinite dilution can be done with reasonable confidence and an estimate of the virial coefficient is also obtained. In addition, optical distortion and base-line errors are somewhat less serious with the low-speed method.

For critical measurements, we prefer to do experiments of both kinds; moreover, all three data plots—$\ln c$ *vs.* r^2, $(dc/dr)/r$ *vs.* c, and M_{app}^{-1} *vs.* c—are prepared for each experiment.

Initial Concentration. The low-speed method requires a separate measurement of c_0, the initial solute concentration,

for reduction of the data by means of a plot of ln c *vs.* r^2. The molecular weight calculated from a $\bar{M}_z$-type plot is independent of the initial concentration. Consequently, a discrepancy between molecular weights found from these plots gives the first warning that there may be some error in the measured c_0. The precise measurement of the initial concentration, c_0, is extremely important, because the error in this value adds algebraically to the local concentration and seriously changes the slope and curvature of the plots. Errors in the measurement of c_0 are, in fact, the chief hazard in the use of the low-speed method for proteins in concentrated guanidinium chloride.

Usually the measurement of c_0 is performed in a synthetic boundary cell. What is actually measured is the difference in refractive indices between the sectors of the cell. This difference is caused not only by the protein but also by any difference there may be between the salt concentrations in the protein solution and the solvent. When the cell is filled, there is great danger that some water will evaporate during the handling of solutions. Let us estimate the error caused by evaporation of 0.01 mg of water/cell load (0.14 ml). The 6 M solution is roughly 50% in guanidinium chloride. Thus, evaporation of 0.07 mg of water/ml of solution changes the concentration of guanidinium chloride by about 0.035 mg/ml. The refractive increment of guanidinuim chloride is about the same as that for proteins, *i.e.*, about 2.9 fringes/mg per ml (as will be shown later). Thus the evaporation of 0.01 mg of water/cell load produces an error of about 0.1 fringe in measurement of c_0. The error is much less in low-density buffers; but even there, it may be appreciable.

After thorough dialysis, extreme care is necessary in handling the solutions and in filling the cell. A dialysis bag can be used if the sample is withdrawn through the cellophane with a syringe and if the bag is not exposed to the air any longer than is absolutely necessary. Evaporation after dialysis is more easily avoided if a plastic dialysis block is used instead of a bag. In either case, the syringe is not emptied into an intermediate container; it is used at once to fill the appropriate channel of a scrupulously cleaned and dried synthetic boundary cell. The remaining contents of the syringe are then used to fill the glass barrel of a disassembled 0.2-ml micrometer syringe from the back. The micrometer is attached to the barrel, leaving no air bubble between the plunger and the solution. The micrometer syringe is then used to load the double-sector cell for the equilibrium run.

When the solutions are treated in this way, the error in the initial concentration should be small, but it still may not be entirely negligible. The time dependence of the apparent c_0 can be used to detect any remaining salt mismatch and to eliminate the salt contribution to the boundary. The solvent components diffuse much faster than the larger molecules of the solute. As a result, there exists a time interval during which the difference of salt concentrations between reference points close to the ends of the solution column decreases appreciably, while the protein boundary is spreading so slowly that the original concentration of the protein at the reference points (*i.e.*, zero and c_0) does not change. The residual salt boundary may be eliminated by extrapolating the apparent c_0 values to infinite time ($1/t = 0$). To check this procedure, we performed a synthetic boundary cell run with two guanidinium chloride solutions with slightly different concentrations (Figure 7). The apparent value of the c_0 at infinite time was negative and its absolute value was about 5% of the zero-time value.

If the solutions are handled carefully, the apparent c_0 value

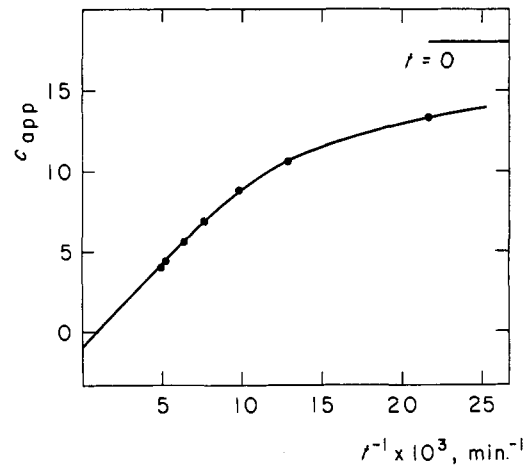

FIGURE 7: The apparent concentration (in fringe units) as a function of reciprocal time. Synthetic boundary cell. Two guanidinium chloride solutions with slightly different concentrations.

should not change with time by more than one fringe. The initial salt boundary is reduced by the above procedure to an error comparable with the experimental scatter of the readings. A large change in the apparent c_0 with time provides a warning that the solution and solvent are badly mismatched and that the experiment must be repeated.

Concentration Units. The fringe count, f, is a convenient concentration unit for experiments in the ultracentrifuge with interference optics. It is proportional to the concentration and in most applications the units of concentration do not matter. It is sometimes useful, however, to be able to convert concentrations measured in fringes to weight concentrations. The fringe count is connected with the concentration by the following relation

$$f = h\Delta n/\lambda = c(\Delta n/c)h/\lambda = Ac \qquad (19)$$

Here h is the thickness of the liquid column, λ is the wavelength of the light under vacuum, and $(\Delta n/c)$ is the refractive index increment of the solute. With $h = 1.2$ cm and $\lambda = 5460$ Å (Wratten No. 77A filter), the proportionality factor $A \equiv (\Delta n/c)h/\lambda$ has a value of 4100 ± 130 ml/g for most nonheme proteins in 0.05 M phosphate buffer (Babul and Stellwagen, 1969). The proportionality constant must be smaller for proteins in concentrated guanidinium chloride, since the refractive index of the complex solvent is considerably higher than that of a dilute buffer.

The refractive index increment $(\Delta n/c)$ is a quantity very similar in character to the specific volume, $\bar{v}$. For multicomponent solvents, the value measured at constant chemical potential should be used. This value depends on the refractive index of the complex solvent and on the preferential sorption of solvent components onto the solute. As the sorption is not known, the proportionality factor has to be measured experimentally.

We have performed this measurement on ovalbumin and serum albumin. Approximately 2% solutions of these proteins in 0.1 M phosphate buffer were diluted on a volume basis (a) into concentrated guanidinium chloride, so that the final concentration was 6 M, and (b) into more of the phosphate buffer. Thus, the pairs of solutions had the same concentration of protein. The concentration of protein (expressed as fringe count) was measured in a synthetic boundary cell against

appropriate solvents. As the solutions were not dialyzed, very careful elimination of the salt boundary by the time-dependence method (see above) was necessary. The ratio of fringe counts for each pair was equal to the ratio of the proportionality factors A(guanidinium)/A(phosphate) and had values of 0.692 and 0.708 for serum albumin and ovalbumin, respectively. This value agrees very well with data from light-scattering experiments (Noelken and Timasheff, 1967). Consequently, the value 2870 was adopted for the proportionality factor A(guanidinium) of proteins in 6 M guanidinium chloride.

Concentration Gradient. For the construction of the $\bar{M}_z$-type plot and of the M_{app}^{-1} plot, the concentration gradients must be measured. For the ith point in the cell, we have calculated dc/dr from interference data according to the relation

$$(dc/dr)_i = (c_{i+1} - c_{i-1})/(r_{i+1} - r_{i-1}) \qquad (20)$$

using the unsmoothed experimental data. The smoothing of data can be dangerous unless it is done very judiciously because one erroneous point may influence many others. The arbitrary elimination of nonfitting points allows the data to appear to be more precise than they really are, and may encourage an unwarranted confidence in the accuracy of the result.

The gradients may, alternatively, be obtained directly from schlieren data and the dependencies constructed from schlieren data are generally smoother. In our experience, however, certain systematic errors are difficult to avoid in measuring the position of the schlieren bar images obtained with a double-sector cell. These errors seem to be particularly serious when the solution and solvent images approach each other closely and when the solution image rises steeply near the bottom of the solution column. In a high-speed run, only a relatively narrow region in the cell provides reliable data. If schlieren data are used, they should be checked against the interference data by plotting

$$f_r - f_{r_0} \; vs. \int_{r_0}^{r} y\,dr$$

where r_0 is an arbitrarily chosen point in the cell and y is the vertical distance between the solution and solvent schlieren bar images. When the plot is not linear with high accuracy, the schlieren data should be rejected.

Matching of Menisci. In loading the two compartments of a double-sector cell, the menisci in the two solution columns may be either matched or deliberately mismatched. For experiments in a mixed solvent—for example, in concentrated guanidinium chloride—we prefer to match the menisci. If the menisci are mismatched in such an experiment, the solvent column should overlap the solution column equally at the two ends. If the menisci are matched, they must be matched precisely; otherwise, the exact positions of the menisci will be obscured. Whichever technique is used, the cell should be filled with a micrometer syringe. In some double-sector cells, the two sectors are not exactly the same; one sector is often slightly farther than the other from the axis of rotation. Thus, the appropriate amounts of base-forming liquid, solvent, and solution must be found for each new centerpiece by preliminary experiments.

Averaging of Data. In each experiment several pictures of the cell were taken, beginning when the solute appeared to be at equilibrium and continuing for at least 24 hr thereafter. The complete calculation was performed for each of these times and the dependences for all of them were plotted in one plot. This revealed immediately whether the system was at equilibrium and helped to eliminate any systematic error in evaluation of a particular picture. This procedure is preferable to evaluating several fringes of the same picture, where possible systematic errors (misalignment of the plate in the comparator, for example) are likely to be the same for all fringes. The constancy of the equilibrium patterns served to show that no solute was being lost by slow aggregation or by interaction with the bottom-forming liquid.

Experimental Section

Materials. Ovalbumin was a two-times-crystallized preparation purchased from Worthington Biochemical Corp., Freehold, N. J. Crystallized and lyophilized bovine serum albumin was purchased from Sigma Chemical Co., St. Louis, Mo. Aspartokinase–homoserine dehydrogenase complex was prepared from *Escherichia coli* 9723 (ATCC) at the Clayton Foundation Biochemical Institute, Department of Chemistry of The University of Texas at Austin by Dr. Willis Starnes (Starnes *et al.*, 1972). Guanidinium chloride was an Ultra Pure grade purchased from Mann Research Laboratories, Orangeburg, N. Y. All other chemicals used for preparation of buffers were analytical grade. Glass-distilled deionized water was used for all solutions.

Buffers and Solutions. The solvent for the sedimentation experiments was 6 M in guanidinium chloride, 0.05 M in dithiothreitol, and 0.1 M in potassium phosphate. The buffer was adjusted to pH 7.0 by potassium hydroxide. About 1 ml of protein solution in 0.05 M phosphate buffer was dialyzed in a cool room for 3–5 days against 50 ml of the guanidinium chloride solution. The concentration was 2–3 mg/ml in low-speed experiments and about 0.5 mg/ml in high-speed ones. The dialysate was used as a solvent in sedimentation experiments.

The density of solvent was measured at 20° in 1-ml pycnometers calibrated with distilled water. The density of the guanidinium chloride solution was in the vicinity of 1.16 g/ml. Duplicate measurements usually agreed to within 0.001 g/ml.

Ultracentrifuge. All experiments were performed at 20° in a Spinco Model E ultracentrifuge equipped with an electronic speed control. Heavy rotors AN-J and AN-H were used for runs at speeds less than 20,000 rpm. At higher speeds, rotors AN-D and AN-H were employed.

Initial Concentration. The aluminum-filled-Epon synthetic boundary cells of the capillary type were filled with 0.14 ml of solution and 0.44 ml of solvent for measurement of the initial concentration. The rotor was brought to 5200 rpm and after the boundary formed and the menisci were matched, the speed was reduced to 4000 rpm. Pictures were taken at regular intervals for 1.5–4 hr. The base-line correction was obtained by removing the rotor after the run, shaking it without removing the cell to destroy the concentration gradient, and accelerating the rotor to 4000 rpm (Richards *et al.*, 1968).

Equilibrium Experiments. Kel F coated aluminum double-sector centerpieces (12 mm) and sapphire windows were used. The cell was filled with approximately 0.05 ml of bottom-forming liquid FC-43 and 0.10 ml of solution and solvent, respectively. The exact amounts were those found by trial to produce matched menisci. The rotor velocities are listed in Tables III and IV. The rotors were kept at speed 80–90 hr in low-speed experiments and 60–70 hr in high-speed experiments. Schlieren and interference pictures were taken once

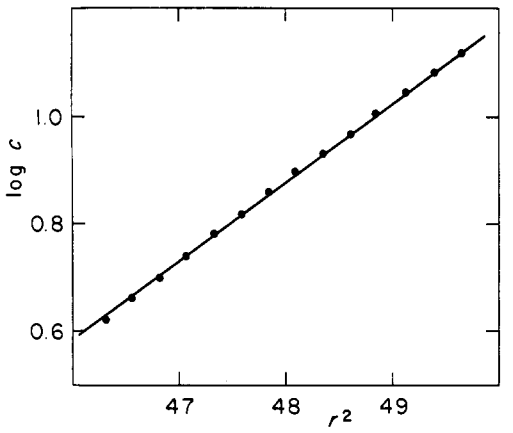

FIGURE 8: Logarithm of concentration (in fringe units) as a function of r^2. Low-speed method for bovine serum albumin in 6 M guanidinium chloride. 83:29 hr at speed.

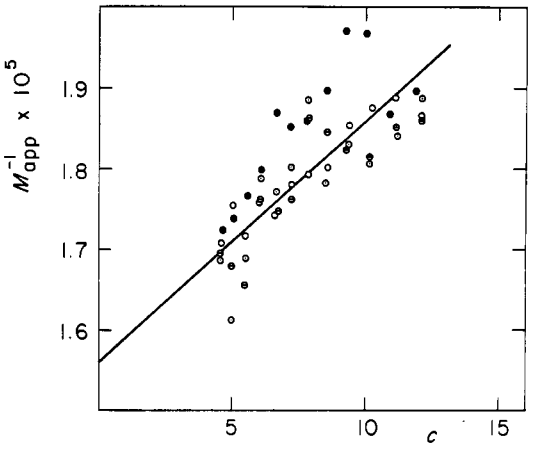

FIGURE 10: $1/M_{app}$ as a function of concentration (in fringe units). Low-speed method. The same equilibrium run as in Figure 8. (●) After 43:25 hr, (○) 66:59 hr, (⊙) 83:28 hr, and (⊖) 83:29 hr.

or twice daily. However, only the interference data were used in final calculations. After each run, the cell was emptied and rinsed without disassembling it. The cell was then filled with water and accelerated to the speed used in the equilibrium experiment. Photographs of the water run were used for baseline corrections (LaBar and Baldwin, 1962).

Plate Reading and Evaluation. For high-speed experiments, the x and y coordinates of a fringe were read on Gaertner microcomparator with a precision of about 0.005 mm (reading "along fringes"). The x coordinates were converted to r values in a standard way; y coordinates, after correction for base line, were used as a measure of concentration. In low-speed experiments, the plates were read either along fringes (for lower total concentrations) or "across fringes" (for higher concentrations, *i.e.*, positions of intersection of a horizontal line with successive fringes were noted). The two methods gave nearly identical results. The measurement was extended as far toward the meniscus and bottom as practicable. The fringe positions at the meniscus and bottom were obtained by extrapolation. These are needed only for calculation of the concentration at the meniscus. Otherwise they do not influence the measurements, and the corresponding points are not included in our plots. The concentration at meniscus was obtained from the initial concentration, c_0, according to the well-known formula (Richards *et al.*, 1968)

$$c_m = c_0 - [r_b^2(c_b - c_m) - \int_{r_m}^{r_b} r^2 dc]/(r_b^2 - r_m^2) \quad (21)$$

For the high-speed experiments, the concentration at the meniscus c_m was chosen in such a way that the low concentration end of the plot log c *vs.* r^2 was straight. This procedure is justified for solutes which are not very heterogeneous (Teller *et al.*, 1969). The value of c_m was usually below 0.010 mm of fringe displacement.

The *density gradient* parameter, Ω, was obtained by equilibrium sedimentation of 6 M guanidinium chloride at 60,000 rpm using schlieren data. The calibration constant was measured in a synthetic boundary cell as described in the literature (Hill and Cox, 1966). The experimental value of Ω was 1.75×10^{-11} (cm^{-5} g) sec^{-2}.

Results and Discussion

We have measured the sedimentation equilibrium of ovalbumin, bovine serum albumin, and aspartokinase–homoserine

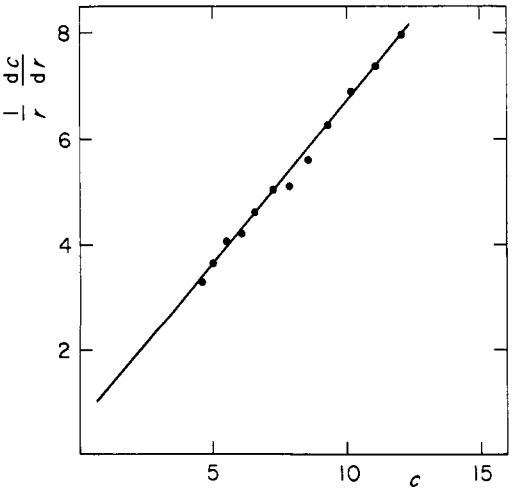

FIGURE 9: $(dc/dr)/r$ as a function of concentration (in fringe units). Low-speed method. The same data as in Figure 8.

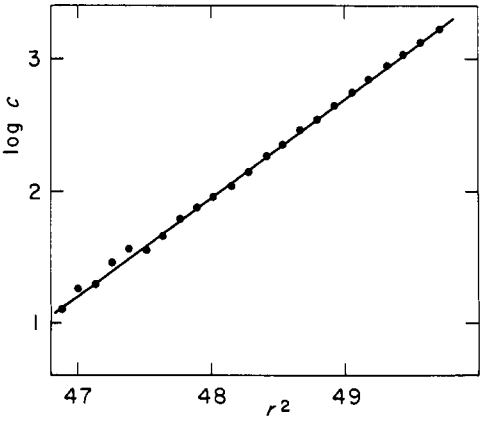

FIGURE 11: Logarithm of concentration (in fringe displacement in mm, 1 fringe = 0.272 mm) as a function of r^2. High-speed method for aspartokinase–homoserine dehydrogenase complex in 6 M guanidinium chloride. 66:10 hr at speed.

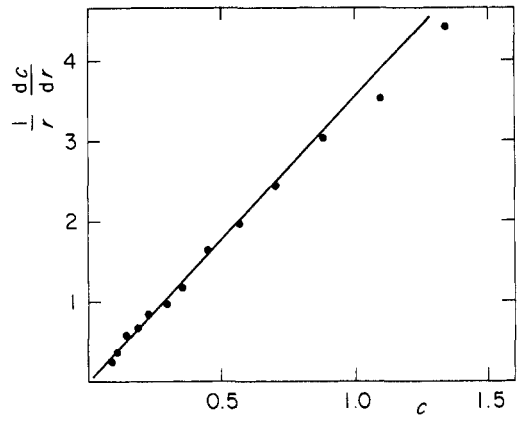

FIGURE 12: (dc/dr)r as a function of concentration (in fringe displacement). High-speed method. The same data as in Figure 11.

dehydrogenase complex in 6 M guanidinium chloride solutions, by both the low-speed and the high-speed methods. Experimental results are summarized in Tables III and IV and some typical data plots are shown in Figures 8–13.

For low-speed experiments, both $\bar{M}_w$ and $\bar{M}_z$ plots (Figures 8 and 9) are curved down so slightly that the plots might appear linear within experimental error if they were not examined closely. Yet the molecular weights calculated from the slopes are quite low, and $\bar{M}_z$ is less than $\bar{M}_w$ just as predicted by the theory for nonideal solutions. The experimental scatter of points in the $1/M_{app}$ *vs.* *c* plot (Figure 10) is exaggerated by the expanded scale of the plot. Actually, a bracket around the least-squares line of ±2000 in molecular weight would include almost all experimental points for times longer than 44 hr. The precision is quite good, considering that the points were obtained using unsmoothed experimental values for point by point evaluation. The extrapolated values of $\bar{M}_w^2/\bar{M}_z$ are appreciably higher than the values obtained from $\bar{M}_w$ and $\bar{M}_z$ plots.

For high-speed experiments the results of the three evaluation techniques differ much less among themselves, but $\bar{M}_z$ still tends to be lower than $\bar{M}_w$. The error caused by the neglect of nonideality is larger than experimental error at least for the aspartokinase subunits which have rather high molecular weight. In all three types of plot, the experimental scattering of points completely masked the curvature of the plots (Figures 11–13) perhaps with the exception of the $\bar{M}_z$ plot (Figure 12). Similar curvature was not observed with the other two

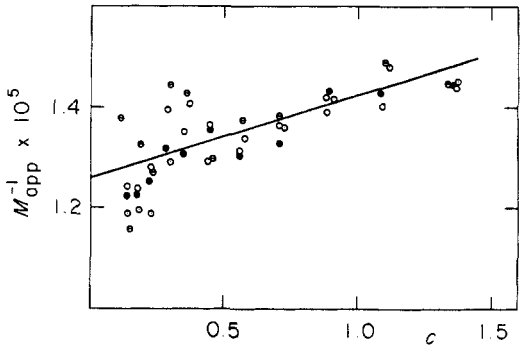

FIGURE 13: $1/M_{app}$ as a function of concentration (in fringe displacement). High-speed method. The same run as in Figure 11. (●) After 40:56 hr, (○) 55:18 hr, (⊙) 66:08 hr, (⊖) 66:10 hr.

TABLE III: Apparent Average Molecular Weights and Virial Coefficients of Several Proteins in 6 M Guanidinium Chloride in Low-Speed Experiments.

	Rpm	$\bar{M}_w$[a]	$\bar{M}_z$[b]	$\bar{M}_w^2/\bar{M}_z$[c]	$B^* \times 10^7$[d]	$B \times 10^3$[e]
Serum albumin	13,000	54,600	49,700	64,200	3.02	0.846
Ovalbumin	16,000	44,700	42,700	47,600	2.85	0.798
Aspartokinase	12,000	63,700	51,500	78,800	3.35	0.939

[a] From slope of ln *c* *vs.* r^2 plot, not corrected for nonideality. [b] From slope of (dc/dr)/r *vs.* *c* plot, not corrected for nonideality. [c] From intercept of $1/M_{app}$ *vs.* *c* plot. [d] From slope of $1/M_{app}$ *vs.* *c* plot in mole/g fringe units. [e] In (mole ml)/g^2 units; it is actually $B + \bar{v}_1\bar{M}_z/\bar{M}_w^2$, but the value of the second term is negligibly small.

proteins. The measurement of the virial coefficient (Figure 13) is quite ambiguous and is much less precise in high-speed experiments than in low-speed experiments due to the low concentration and the related scatter of experimental points in the $1/M_{app}$ *vs.* *c* plot.

All the above calculations were performed without applying the density gradient corretion. When the correction was applied to the low-speed experiment on serum albumin, the molecular weight increased by about 0.05% and the virial coefficient by about 0.4%. For high-speed experiments there was a 0.01% increase in molecular weight and 3% increase in virial coefficient. These corrections are completely negligible compared to the experimental error.

The extrapolated values obtained for the molecular weight $\bar{M}_w^2/\bar{M}_z$ by the high-speed and low-speed methods agree quite well with each other. The measured molecular weights for ovalbumin and serum albumin also agree reasonably well with the accepted values for these proteins. Part of the difference is without doubt caused by the uncertainty in the value of apparent specific volume $\bar{v}_1^*$. Due to the higher density of guanidinium chloride solutions, the error that would be caused by an erroneous value of $\bar{v}_1^*$ is about twice as large as for dilute buffers under similar conditions. In our computations we have used for $\bar{v}_1^*$ the averaged literature values of $\bar{v}_1$ in dilute buffers reduced by 0.010, *i.e.*, 0.722, 0.739, and 0.725 ml per g for serum albumin, ovalbumin and aspartokinase, respectively. The experiment with aspartokinase is one of those reported in the accompanying paper (Starnes *et al.*, 1972). The molecu-

TABLE IV: Apparent Average Molecular Weights and Virial Coefficients of Several Proteins in 6 M Guanidinium Chloride in High-Speed Experiments.[a]

	Rpm	$\bar{M}_w$[a]	$\bar{M}_z$[b]	$\bar{M}_w^2/\bar{M}_z$[c]	$B^* \times 10^7$[d]	$B \times 10^3$[e]
Serum albumin	26,000	64,000	64,700	66,700	1.63	0.467
Ovalbumin	36,000	48,000	46,800	48,900	4.22	1.180
Aspartokinase	26,000	74,500	74,000	79,200	4.45	1.246

[a–e] See Footnotes to Table III.

lar weight corresponds to four subunits per molecule of native enzyme in agreement with other evidence presented in that paper and in contrast to some older data which did not take into account the nonideality of the system (Truffa-Bachi *et al.*, 1969).

The second virial coefficients have similar values for all three proteins. These values are about one-half of the values obtained by osmotic measurements (Lapanje and Tanford, 1967; Castellino and Barker, 1968). (Note the difference in definitions of osmotic and sedimentation virial coefficients.) This discrepancy may be explained either by the slight difference in the composition of solvent (*i.e.*, dithiothreitol *vs.* β-mercaptoethanol) or more likely by the residual heterogeneity of proteins that would lower the apparent value of the virial coefficients.

Conclusions

Denatured solutions of proteins in 6 M guanidinium chloride are highly nonideal. Simulated experiments show that, in these systems, the evaluation of sedimentation equilibrium data by means of conventional $\bar{M}_w$- and $\bar{M}_z$-type plots can yield erroneous data even if the appearance of the plots is not obviously anomalous. The error is substantial for the low-speed method and may not be negligible for the high-speed method. The $1/M_{app}$ *vs.* c plot yields $\bar{M}_w^2/\bar{M}_z$ as the reciprocal intercept; the slope of this plot is a combination of the second virial coefficient and a heterogeneity term. Heterogeneity introduces curvature into this plot and lowers the average slope of the curve.

The experimental results have confirmed the theoretical deductions. Thus only methods which eliminate nonideality are applicable when using the more precise low-speed method. Plots of $1/M_{app}$ *vs.* c yield molecular weights with reasonable accuracy and give estimates of second virial coefficients. These estimates tend to be lower than the values obtained by other methods, probably due to the interference of residual heterogeneity of the samples.

At the lower concentrations used for the high-speed method, the effect of nonideality is less. Simultaneously, the effect of sample heterogeneity increases due to the higher speed. The slope of the plot of $1/M_{app}$ *vs.* c should be a sensitive indicator of heterogeneity. Consequently, the improvement achieved by the use of this plot is not so large for high-speed experiments. Nevertheless, the error committed by neglecting the nonideality can be well above the experimental error. In general, molecular weights measured in guanidinium chloride by the high-speed method should be expected to be a little low.

The effect of the density gradient is completely negligible for protein solutions in guanidinium chloride. It may be important for solutions of other salts (*e.g.*, cesium salts) which have a much higher value of the density gradient parameter, Ω.

Acknowledgment

We thank Dr. Willis Starnes for a sample of aspartokinase–homoserine dehydrogenase complex.

References

Babul, J., and Stellwagen, E. (1969), *Anal. Biochem. 28*, 216.
Casassa, E. F., and Eisenberg, H. (1964), *Advan. Protein Chem. 19*, 287.
Castellino, F. J., and Barker, R. (1968), *Biochemistry 7*, 2207.
Deonier, R. C., and Williams, J. W. (1969), *Proc. Nat. Acad. Sci. U. S. 64*, 828.
Fujita, H. (1962), Mathematical Theory of Sedimentation Analysis, New York, N. Y., Academic Press.
Goldberg, R. J. (1953), *J. Phys. Chem. 57*, 194.
Green, R. W., and McKay, R. H. (1969), *J. Biol. Chem. 244*, 5034.
Hill, J., and Cox, D. J. (1966), *J. Phys. Chem. 70*, 2946.
Kawahara, K., and Tanford, C. (1966), *Biochemistry 5*, 1578.
LaBar, F. E., and Baldwin, R. L. (1962), *J. Phys. Chem. 66*, 1952.
Lapanje, S., and Tanford, C. (1967), *J. Amer. Chem. Soc. 89*, 5030.
Noelken, M. E., and Timasheff, S. N. (1967), *J. Biol. Chem. 242*, 5080.
Reisler, E., and Eisenberg, H. (1969), *Biochemistry 8*, 4572.
Richards, E. G., and Schachman, H. K. (1959), *J. Phys. Chem. 63*, 1578.
Richards, E. G., Teller, D. C., and Schachman, H. K. (1968), *Biochemistry 7*, 1054.
Roark, D. E., and Yphantis, D. A. (1969), *Ann. N. Y. Acad. Sci. 164*, 245.
Seery, V. L., Fisher, E. H., and Teller, D. C. (1967), *Biochemistry 6*, 3315.
Seery, V. L., Fisher, E. H., and Teller, D. C. (1970), *Biochemistry 9*, 3591.
Starnes, W. L., Munk, P., Maul, S. B., Cunningham, G. N., Cox, D. J., and Shive, W. (1972), *Biochemistry 11*, 677.
Tanford, C. (1961), Physical Chemistry of Macromolecules, New York, N. Y., John Wiley and Sons.
Tanford, C., Kawahara, K., and Lapanje, S. (1967), *J. Amer. Chem. Soc. 89*, 729.
Teller, D. C., Horbett, T. A., Richards, E. G., and Schachman, H. K. (1969), *Ann. N. Y. Acad. Sci. 164*, 66.
Truffa-Bachi, P., van Rapenbusch, R., Janin, J., Gros, C., and Cohen, G. N. (1969), *Eur. J. Biochem. 7*, 401.
Yphantis, D. A. (1964), *Biochemistry 3*, 297.